

Published in final edited form as:

Cancer Res. 2010 September 1; 70(17): 6849–6858. doi:10.1158/0008-5472.CAN-10-0790.

SG2285, a novel C2-aryl-substituted pyrrolobenzodiazepine dimer pro-drug that cross-links DNA and exerts highly potent antitumor activity

John A. Hartley^{1,2,*}, Anzu Hamaguchi¹, Marissa Coffils¹, Christopher R.H. Martin¹, Marie Suggitt¹, Zhizhi Chen³, Stephen J. Gregson³, Luke A. Masterson³, Arnaud C. Tiberghien³, Janet M. Hartley², Christopher Pepper⁴, Thet Thet Lin⁴, Christopher Fegan⁴, David E. Thurston³, and Philip W. Howard³

¹Spirogen Ltd, UCL Cancer Institute, Paul O’Gorman Building, 72 Huntley Street, London WC1E 6BT, UK

²CR-UK Drug-DNA Interactions Research Group, UCL Cancer Institute, Paul O’Gorman Building, 72 Huntley Street, London WC1E 6BT, UK

³Spirogen Ltd, 29/39 Brunswick Square, London WC1N 1AX, UK

⁴Dept. Haematology, Cardiff University, Cardiff CF14 4XN, UK

Abstract

The pyrrolobenzodiazepines (PBDs) are naturally occurring antitumor antibiotics and a PBD dimer (SJG-136, SG2000) is in Phase II trials. Many potent PBDs contain a C2-*endo-exo* unsaturated motif associated with the pyrrolo C-ring. The novel compound SG2202 is a PBD dimer containing this motif. SG2285 is a water-soluble pro-drug of SG2202 in which two bisulphite groups inactivate the PBD N10-C11 imines. Once the bisulphites are eliminated, the imine moieties can bind covalently in the DNA minor groove forming an interstrand cross-link. The mean *in vitro* cytotoxic potency of SG2285 against human tumour cell lines is GI₅₀ 20 pM. SG2285 is highly efficient at producing DNA interstrand cross-links in cells, but they form more slowly than those produced by SG2202. Cellular sensitivity to SG2285 was dependent primarily on ERCC1 and homologous recombination repair. In primary B-CLL samples the mean LD₅₀ was significantly lower than in normal age-matched B- and T-lymphocytes. Antitumor activity was demonstrated in several human tumor xenograft models, including ovarian, non-small cell lung, prostate, pancreatic and melanoma, with cures obtained in the latter model with a single dose. Further, in an advanced stage colon model, SG2285 administered either as a single dose, or in two repeat dose schedules, was superior to irinotecan. Our findings define SG2285 as a highly active cytotoxic compound with antitumor properties desirable for further development.

INTRODUCTION

The pyrrolo[2,1-*c*][1,4]benzodiazepines (PBDs) are a family of naturally occurring antitumor antibiotics produced by *Streptomyces* species (1). The PBD monomers, which include anthramycin and sibiromycin, exert their biological activity by binding in the minor

*To whom correspondence should be addressed: Professor John A Hartley, UCL Cancer Institute, Paul O’Gorman Building, University College London, 72 Huntley Street, London, WC1E 6BT, Tel: +44 (0) 20 7679 6055, Fax: +44 (0) 20 7679 6925, john.hartley@ucl.ac.uk.

Note:

SG2285 is owned by Spirogen Ltd in which J.A. Hartley, P.W. Howard and D.E. Thurston have equity interests. The data contained in this paper have been presented in part at the annual meeting of the American Association for Cancer Research in 2008 (32).

groove of DNA with a selectivity for 5'-purine-G-purine sequences, forming a covalent bond to the exocyclic amino group of the guanine base (2). PBD dimers have been designed and synthesized, by joining two monomer PBD units together through their C8-positions via a flexible linker (3-7). This has resulted in molecules capable of recognising longer sequences of DNA (e.g. 5'-purine-GATC-pyrimidine, see Supplementary Material section S1) and producing highly cytotoxic, non-distorting DNA interstrand cross-links in the DNA minor groove (8-11). One such dimer, SJG-136 (SG2000, Figure 1A), was demonstrated to have significant *in vitro* and *in vivo* antitumor activity (11,12). It has recently completed Phase I clinical trials in the UK (through Cancer Research UK (13)) and in the USA (through NCI (14,15)) and is about to enter Phase II studies against both solid tumors and hematological malignancies.

Many of the most potent naturally occurring PBD monomers have *endo/exo*-unsaturation at the C2 position. Synthetic PBD monomers that retain this motif have established that C2-unsaturation enhances *in vitro* potency (16). This finding has now been applied to PBD dimers with the synthesis of SG2202 (17, Figure 1A) where two PBD monomer units, which retain the *endo-exo* unsaturation motif in the form of a C2-aryl substituent conjugated to a 2,3 double bond, are joined via their C8/C8' positions through a propyldioxy linker. This molecule had significantly greater *in vitro* cytotoxicity (17) compared to the C2-unsaturated parent molecule (DSB-120 (8)), or to SJG-136 (11). The additional C2/C2'-aryl substituents, however, lowered water solubility to a level that made further development of this compound challenging.

Therefore, SG2202 was converted into the C11/C11' bisulfite adduct resulting in SG2285 (Figure 1A (17)) whereby the two bisulphite groups inactivate the N10-C11 imines of the PBD units. The pro-drug exists in two predominant diastereomer forms, 11*S*,11'*R* and 11*S*,11'*S* (Figure 1A). Once the bisulphite groups are eliminated to produce SG2202, the two PBD imine moieties are able to bind covalently in the minor groove of DNA to the N2-positions of guanine on opposite strands of DNA to form an interstrand cross-link (Figure 1B). SG2285 is freely water soluble and stable in aqueous conditions, retaining the *in vitro* potency of SG2202 (17). Using plasmid DNA in an agarose gel electrophoresis assay, SG2285 was found to be a highly efficient DNA interstrand cross-linking agent (17). Cross-links, however, formed more slowly than those produced by the parent molecule SG2202, reaching a peak at 2 hours for SG2202 and >18 hours for SG2285, confirming that it behaves as a pro-drug.

The current study documents the *in vitro* activity of SG2285 and confirms its DNA interstrand cross-linking ability in human tumor cells. Potent activity in primary B-CLL (both from untreated and previously treated patients) and apoptosis induction through the intrinsic pathway are demonstrated. In addition, potent antitumor activity is demonstrated against a wide range of *in vivo* human solid tumor xenograft models using different dosing schedules, providing a clear rationale for further pre-clinical development of this novel agent.

MATERIALS AND METHODS

Drugs

SG2202 and pro-drug SG2285 were synthesised as previously described (17). Different batches of SG2285 containing different 11*S*,11'*R* and 11*S*,11'*S* diastereomeric ratios were used in the current study. The ratios of 11*S*,11'*S*: 11*S*,11'*R* for batches 2-5 are 1:1.87, 1:5.1, 26.5:1, and 1:9, respectively. The ratio for batch 1 was not determined.

Cell lines

All human tumor cell lines were obtained between 2003 and 2008 from the American Type Culture Collection (ATCC) or the European Collection of Cell Cultures (ECACC) with the exception of LOX-IMVI and OVCAR-5 which were obtained in 2004 from the Developmental Therapeutics Program, National Cancer Institute.

The Chinese hamster ovary AA8, UV23, UV47, UV61 and UV96 cell lines were obtained in 1998 from Dr. M. Stefanini Istituto di Genetica Biochimica et Evoluzionistica, Pavia, Italy). V79, irs1, irs1SF, CHO-K1, xrs5 cell lines were kindly provided in 1998 by Prof. J. Thacker (MRC Radiation and Genome Stability Unit, Harwell, UK). UV135 was obtained in 1998 from ATCC (No CRL-1867).

All cell lines were kept at low passage, returning to original frozen stocks every 3-6 months, and tested regularly for mycoplasma. The lines have not been re-authenticated since receipt.

Growth Inhibition assays

For growth inhibition assays in human tumour cell lines 190 μ l cell suspension was added to each well of a 96 well plate (haematological lines at 5×10^4 cells / ml, all other lines at 1×10^4 cells / ml). Following drug addition plates were incubated for four control cell doublings, Following incubation (with the exception of OVCAR-5 and HT29 cells), Alamar Blue, which stains living cells, was added to each well to a final concentration of 1 μ M. For OVCAR-5 and HT29, MTT solution to a final concentration of 1.5 μ M was added to each well. Plates were then incubated for a further 4 hours, with the exception of U266B1 cells (5 hours) and HCT-8 cells (2 hours), at 37°C. Plates were read using an Envision plate reader and data analysed using GraphPad Prism, and GI₅₀ values obtained.

Studies in Chinese hamster ovary (CHO) cells were performed using the SRB assay as previously described (18).

Measurement of DNA Interstrand Cross-linking in Cells Using the Single Cell Gel Electrophoresis (Comet) Assay

Exponentially growing DU145 cells were plated onto 2 \times 6 well plates at 3×10^4 /mL (2mL/well) and incubated at 37°C overnight to allow the cells to adhere. The following day medium was removed and replaced with serum-free medium containing SG2285 at 1 nM. The plates were then incubated at 37°C and cells harvested at 0, 4, 8, 16, 24 and 32 hours. The cells were stored at -80°C until assayed for cross-linking using the modified single cell gel electrophoresis (comet) assay as previously described (19,20).

Comets were analysed using a Nikon inverted fluorescent microscope and Kinetic Imaging software (KOMET version 4). The tail moments (TM) of 25 cells/slide were measured and the mean tail moment of duplicate slides calculated. The mean resultant TM (Res TM) for each dose was calculated as TM of irradiated cells – TM of un-irradiated cells. The percent decrease in TM was calculated by the equation:

$$\% \text{ decrease in TM} = [1 - (\text{Res TM of drug treated} / \text{Res TM control})] \times 100$$

Studies in B-CLL

Peripheral blood samples from 20 patients with B-CLL were obtained with the patients' informed consent. B-CLL was defined by clinical criteria as well as cellular morphology and the co-expression of CD19 and CD5 in lymphocytes simultaneously displaying restriction of

light-chain rearrangement. None of the previously treated patients ($n = 10$) had received therapy for at least two months prior to this study.

Freshly isolated peripheral blood lymphocytes from B-CLL patients and normal age-matched controls as well as AML cell lines (1×10^6 /mL) were cultured in RPMI medium (Invitrogen, Paisley, UK) supplemented with 100 units/ml penicillin, 100 μ g/ml streptomycin and 10% fetal calf serum. Cells were incubated at 37°C in a humidified 5% carbon dioxide atmosphere in the presence of SG2285 (10^{-10} - 10^{-7} M) for time points up to 48 h. Cells were harvested by centrifugation and then re-suspended in 195 μ L of calcium-rich buffer. Subsequently, 5 μ L of Annexin V (Caltag Medsystems, Botolph Claydon, UK) was added to the cell suspension and cells were incubated in the dark for 10 mins prior to washing. Cells were finally re-suspended in 190 μ L of calcium-rich buffer together with 10 μ L of propidium iodide. Apoptosis was assessed by dual-colour immunofluorescent flow cytometry.

To measure SG2285-induced caspase-3 activation, cells were harvested by centrifugation and labeled with CD19 APC conjugated antibody. Subsequently the cells were incubated for 1h at 37°C in the presence of the PhiPhiLux™ G₁D₂ substrate (Calbiochem, Nottingham, UK) which contains two fluorophores separated by a quenching linker sequence that is cleaved by active caspase-3. Once cleaved, the resulting products fluoresce green and can be quantified using flow cytometry. In additional experiments the caspase-8 inhibitor, Z-IETD-FMK, or the caspase-9 inhibitor, Z-LEHD-FMK, (Cambridge Bioscience, Cambridge, UK) were added to SG2285-treated cell cultures (final concentration 2 μ M) in order to determine whether either of these inhibitors was able to abrogate the apoptotic effects of SG2285 in CLL cells.

Data were evaluated using the Student's *t*-test or Mann-Whitney test and correlation coefficients were calculated from least squares linear regression plots. Drug sensitivity was evaluated using non-linear regression and line of best-fit analysis of the sigmoidal dose-response curves. All statistical analyses were performed using Graphpad Prism 3.0 software.

In Vivo Studies

LOXIMVI Melanoma and OVCAR-5 Ovarian Tumours—UKCCCR guidelines for the welfare of animals in experimental neoplasia were adhered to throughout the study.

Tumor fragments of less than 3 mm were implanted subcutaneously into the left or right flanks of the mice, and tumour growth was monitored as the relative tumor volume (RTV). Tumor volume was calculated using the formula: Tumor volume = $(w^2 \times l) / 2$, where w is the width and l the length of the tumor. RTV was calculated using the formula: RTV = Tumor volume day n / Tumor volume day 0. Animals were sorted into treatment groups with mean tumor volumes of 64 mm³.

SG2285 was administered i.v. as a single dose, in volumes of 0.1 mL per 10 g body weight. Control groups received vehicle only. Percentage tumour growth delay (% TGD) was calculated using the formula: % TGD = [Time (days) taken to reach endpoint (treatment group) – Time (days) taken to reach endpoint (control group)] / Time (days) taken to reach endpoint (control group) \times 100. The endpoint was defined as the tumor reaching 17 mm in length. Treatment outcome was evaluated by % TGD and complete regression (CR).

Advanced LS174T Colon and SKOV-3 Ovarian Tumors—LST174 xenografts were initiated from tumors maintained in *nu/nu* mice. SK-OV-3 xenografts were initiated from tumors maintained in severe combined immunodeficiency (SCID) mice. Tumor fragments of 1 mm were implanted subcutaneously into the right flanks of test mice (*nu/nu* for LS174T

and SCID for SK-OV-3). AAALAC guidelines for animal care and use were adhered to throughout the study. Animals were sorted into treatment groups with mean tumor volumes of 323 to 326 mm³ (LST174) and 99.9 to 100 mm³ (SK-OV-3). Compound in 5% DMA/95% physiological saline was administered at various dosing regimens, in volumes of 0.1 ml per 10g body weight. For LST174, one group received Irinotecan intraperitoneally (i.p.) qwk x3. Control groups received vehicle only. The endpoint was defined as the tumors reaching 1500 mm³ or 69 days for LST174, 2000 mm³ or 79 / 120 days for SK-OV-3. Treatment outcome was evaluated by % TGD and CR.

LS174T Colon, A549 NSCLC, PC3 Prostate and Bx-PC-3 Pancreatic

Tumors: LST174, PC3 and Bx-PC-3 xenografts were initiated from tumors maintained in *nu/nu* mice. A549 xenografts were initiated from cultured cells maintained in Kaighn's modified Ham's F12 medium supplemented with 10% fetal bovine serum, 100 units/mL penicillin, 100 µg/mL streptomycin sulphate, 25 µg/mL gentamycin, 2 mM glutamine and 1 mM sodium pyruvate. Tumor fragments of 1 mm were implanted subcutaneously into the right flanks of test mice. For A549 xenografts, cells were harvested during log phase and re-suspended in 50% Matrigel matrix (BD biosciences) at 5×10^7 cells/ml. Each mouse was injected subcutaneously in the right flank with 1×10^7 cells (0.2 ml cell suspension).

Animals were sorted into treatment groups with mean tumor volumes of 99 to 100 mm³ (LST174), 128 to 130 mm³ (A549), 106 to 107 mm³ (PC3) and 105 to 107 mm³ (Bx-PC-3). SG2285 in 33% propylene glycol/5% dextrose was administered at various dosing regimens, in volumes of 0.1 ml per 10 g body weight. For LST174, one group received Irinotecan at 100 mg / kg (i.p.) qwk x3 and one group received 5-FU at 100 mg / kg, i.p. qwk x3. For A549, one group received Docetaxel at 30 mg / kg, i.v. q4d x3. For PC3, one group received Paclitaxel at 30 mg / kg i.v. qod x5 and one group received cisplatin at 10 mg / kg i.p. qwk x3. For Bx-PC-3, one group received Paclitaxel at 30 mg / kg, i.v. qod x5. Control groups received vehicle only. The endpoint was defined as the tumor reaching 2000 mm³ in the control group or 26 days (LST174), 29 days (A549) and 30 days (Bx-PC-3). For PC3, the study was terminated at 30 days. Treatment outcome was evaluated by % tumor growth inhibition (% TGI) and partial regression (PR). %TGI was calculated using the formula: % TGI = ((median final tumor volume_{control} – median final tumor volume_{treated}) / median final tumor volume_{control}) × 100. An agent that produced at least 60 %TGI was considered to be potentially therapeutically active. PR was indicated by tumor volumes 50 % or less than the volume at day 1 of treatment.

RESULTS

SG2285 is the C11/C11' bisulfite adduct pro-drug of SG2202 which exists in two main diastereomeric forms, 11*S*,11'*R* and 11*S*,11'*S* (Figure 1A). The active drug spans eight base pairs in the minor groove of DNA (Figure 1C), forming interstrand cross-links between guanine N2 positions spanning four base pairs as depicted in Figure 1B.

Activity of SG2285 In Vitro

The *in vitro* activity of SG2285 was determined following continuous exposure in a panel of human tumor cell lines (Figure 2A). The average GI₅₀ across the panel was 20 pM, range 0.3 pM (HL-60) to 68 nM (HCT-15). These data confirm the potent *in vitro* activity of SG2285 against both hematological and solid tumor cell lines. In addition, the 10⁴ range in GI₅₀ values among the cell lines suggests that this agent confers a multilog, differential effect upon cell lines rather than exerting a non-specific cytotoxicity. (For a comparison with other DNA cross-linking agents see Supplementary Material section S2, Table S1).

The activity of SG2285 was also determined in a panel of Chinese hamster ovary (CHO) cell lines with defined defects in specific DNA repair pathways (Table 1). Cell lines defective in the nucleotide excision repair (NER) genes XPB, XPG, XPF and CSB showed a modest increase in sensitivity (1.2 – 3.2 fold) over wild-type cells. Cells defective in the non-homologous end joining (NHEJ) Ku 70 subunit (XRCC5) showed no increased sensitivity. In contrast, cells defective in the NER factor ERCC1 showed a 12.1-fold increased sensitivity to SG2285. In addition, cells defective in the RAD51 paralogs XRCC2 and XRCC3 were highly sensitive to SG2285 with 16.7 and 10.9-fold increased sensitivities, respectively. These data suggest that cellular sensitivity of the minor groove cross-linking agent SG2285 is dependent on ERCC1 and homologous recombination repair.

DNA Interstrand Cross-linking by SG2285 in Cells

We have previously shown SG2285 to efficiently cross-link naked DNA (17) with the cross-links forming more slowly than with SG2202. DNA interstrand cross-linking was determined in the human prostate cancer cell line DU145 treated with 1 nM SG2285 using the single cell gel electrophoresis (comet) assay (Figure 2B). Cross-links form slowly, with none evident in the initial 4 hours. A significant level of cross-linking was observed at 8 hours, which was still increasing at 32 hours. This is in contrast to other PBD dimers such as SJG-136 where cross-links form rapidly in cells with the majority forming within the first few hours of exposure (11). These data are therefore consistent with SG2285 acting as a pro-drug, slowly releasing the highly potent cross-linking agent SG2202.

Study of SG2285 in Primary B-CLL Cells

In vitro drug sensitivity was measured in 20 primary B-CLL samples using the Annexin V/propidium iodide assay and LD₅₀ values were calculated. Apoptosis was induced in all 20 patient samples following exposure to SG2285 with a mean LD₅₀ value (\pm SD) of 8.3 (\pm 3.4) $\times 10^{-9}$ M (Figure 3A) and LD₉₀ value 4.6 (\pm 2.4) $\times 10^{-8}$ M. Normal B- and T-lymphocytes from ten age-matched controls demonstrated higher LD₅₀ values than the B-CLL cells ($P < 0.0001$ and $P < 0.0001$, respectively, Figure 3A). This difference was not observed with the cross-linking agent chlorambucil, where the normal cells were found to be more sensitive (Figure 3A)

The development of drug resistance in B-CLL is associated with previous treatment and is often pleiotropic in nature (21). In this study, we compared SG2285 LD₅₀ values between previously treated ($n = 10$) and untreated ($n = 10$) patient groups (Figure 3B). There was a trend towards increased resistance to SG2285 in the previously treated group but this did not reach statistical significance ($P = 0.07$), whereas the increase was significant with chlorambucil ($P = 0.003$).

Aliquots of B-CLL cells were exposed to 5 nM or 10 nM SG2285 for up to 72 h. Apoptosis induction was dose-related and increased significantly between 36 and 48 hours, and was still increasing at 72 hours (Figure 3C). DNA interstrand cross-linking in B-CLL cells was evaluated at 2 nM. Consistent with the apoptosis induction, and the data in Figure 2B, cross-links formed slowly and were only evident after 8 hours, still increasing at 48 hours (see Supplementary Material section S3, Figure S1).

In order to elucidate the exact caspase activation pathway that SG2285 employs in B-CLL cell killing, a series of experiments were performed using caspase inhibitors in order to evaluate their ability to block SG2285-induced apoptosis (Figure 3D). The pan caspase inhibitor Z-VAD.fmk at a concentration of 2 μ M significantly inhibited the cytotoxic effects of SG2285. The caspase-9 inhibitor (LEHD.fmk) also caused a reduction in SG2285-induced apoptosis at a final concentration of 2 μ M, but the caspase-8 inhibitor (IETD.fmk)

had little cytoprotective effect as shown in Figure 3D. Therefore, SG2285 induces apoptosis through the intrinsic apoptotic pathway.

Antitumor Activity of SG2285 In Vivo

The antitumor activity of SG2285 was evaluated in a range of human tumor xenograft models using different i.v. dosing schedules. Representative experiments are shown in Figure 4 and data from all experiments are summarized in Table 2. In an early stage melanoma LOX-IMVI, which was previously shown to be sensitive to SJG-136 (11), a single administration of SG2285 at 3 mg/kg gave 7/7 tumor-free survivors at the end of the study period (day 68, Figure 4A, Table 2A). A further study gave 8/8 tumor-free survivors at day 86, with single doses of 1.5 and 0.75 mg/kg giving 6/8 and 4/8 tumor-free survivors, respectively. Activity was also observed in the ovarian OVCAR-5 model following a single administration of 3 mg/kg (% tumor growth delay (TGD) = 59) although no tumor-free survivors or complete responses were seen in this model (Table 2A).

In an advanced LS174T colon model (mean tumor volume $>300\text{mm}^3$ at start of treatment) SG2285 was also effective following a single administration of 4 mg/kg (Figure 4B) giving %TGD of 138 (Table 2A). Improved efficacy was observed using repeated schedules of 1.5 mg/kg q4dx3 or 0.8 mg/kg qdx5 (Figure 4B) giving %TGD values of 219 and 202, respectively. In this model SG2285 was considerably more efficacious than irinotecan at a standard dose of 100 mg/kg i.p. qwkx3 (%TGD = 54, Figure 4B). In the SKOV-3 ovarian cancer model SG2285 was highly effective using a q4dx3 schedule at doses of 0.5, 0.25 and 0.1 mg/kg (Figure 4C) giving %TGD values of 325, 309 and 325, respectively (Table 2A). At the top dose 8/9 of the animals were still alive at the end of the experiment (120 days). In contrast, with the standard agent cisplatin at 8 mg/kg qwkx3 all animals had to be sacrificed by day 92 (Figure 4C). Further experiments in this model confirmed the potent activity of SG2285 using both a q4dx3 schedule and a qdx5 schedule with tumor-free survivors observed at 0.375 and 1.5 mg/kg (q4dx3) and 0.4 and 0.8 mg/kg (qdx5) (Table 2A). Comparison in this model between different batches of drug containing different 11*S*,11'*R* and 11*S*,11'*S* diastereomer ratios ranging from 1:1.87 (batch 2) to 26.5:1 (batch 4) confirmed activity in all cases (Table 2A).

Significant activity was also observed in a series of shorter duration *in vivo* experiments (26-30 days) using 100 mm³ tumors (Table 2B). SG2285 at 0.85 and 1 mg/kg qd4x3 was superior to irinotecan (100 mg/kg qwkx3 i.p.) and 5-FU (100 mg/kg qwkx3 i.p.) in the LS174T colon model. SG2285 (1 mg/kg qd4x3), although producing a significant tumor growth delay, was less active than docetaxel (30 mg/kg qwkx3) in the non-small cell lung cancer model A549 (%TGI 63 and 89, respectively). In the PC3 prostate model SG2285 gave 5/10 and 4/10 partial responses at 0.75 qd4x4 and 1.0 mg/kg qd4x3, respectively, which was superior to cisplatin (10 mg/kg qwkx3 i.p., no partial responses) but less active than paclitaxel (30 mg/kg qodx5, 8/10 partial responses). Finally, SG2285 gave partial responses in the Bx-PC-3 prostate cancer model whereas none were seen with paclitaxel.

DISCUSSION

SG2202 is the first example of a C2/C2'-aryl PBD dimer which has been converted to a stable, highly water soluble pro-drug form (SG2285) by conversion to C11/C11'-bisulphite diastereomers. SG2285 retains the *in vitro* potency of SG2202 (17). The formation of DNA interstrand cross-links by SG2285 is significantly delayed compared to SG2202 both in naked DNA (17) and in intact cells. In both cases a similar level of cross-linking is eventually achieved, consistent with SG2285 acting as a prodrug and releasing the bisulphite groups to provide a slow conversion to the active PBD dimer SG2202.

SG2285 is more potent *in vitro* than SJG-136, the first PBD dimer to enter clinical trials. For example, the mean GI₅₀ in the panel of human tumor cell lines (Figure 2) was 20 pM compared to 7.4 nM for SJG-136 in the NCI 60 cell line panel (11). Consistent with this increased potency is the approximately 50-fold lower concentration of SG2285 required to produce an equivalent level of DNA interstrand cross-linking in cells.

The data obtained in the panel of DNA repair-defective CHO mutants indicated that sensitivity to SG2285 was primarily dependent on ERCC1 and homologous recombination (XRCC2 and 3 (22-25)). With conventional cross-linking agents such as nitrogen mustards and platinum drugs the XPF-ERCC1-specific nuclease has been demonstrated to play a critical role in repair or 'unhooking' of interstrand cross-links both in cell free systems and in cells (26-28). We have previously shown in the same panel of cell lines that sensitivity to SJG-136 was increased 7.5-fold in both XPF and ERCC1 defective cells (18). Interestingly, for SG2285 the level of sensitivity in ERCC1 (12.1-fold) was much higher than for XPF (3.1-fold), suggesting a greater dependence on ERCC1. This has not been observed previously for other cross-linking agents. Consistent with other cross-linking agents, however, including SJG-136, is the highly increased sensitivity (11- and 17-fold) of SG2285 in XRCC2 and XRCC3 cells, confirming the importance of homologous recombination repair in the processing of unhooked and re-sectioned interstrand cross-links (18, 27-29).

Potent *in vitro* activity was also confirmed in primary B-CLL samples with an LD₅₀ value more than two logs lower than fludarabine, the current treatment choice for this condition, and lower than SJG-136 (30). Importantly, SG2285 exhibited significant differential apoptotic activity (by the intrinsic apoptotic pathway) between normal B and T lymphocytes, and B-CLL cells. In addition, leukemic cells isolated from previously treated patients were not more resistant to SG2285 compared to those isolated from treatment naïve patients. Taken together these data indicate that SG2285 might be a useful option for the treatment of this hematological malignancy which remains incurable with a median survival for advanced stage patients of only three years (31).

SG2285 was found to be a highly active antitumor agent *in vivo*, with activity observed in all models tested. Complete regressions and tumor-free survivors were observed in the LOX-IMVI melanoma and SKOV-3 ovarian models, and tumor regressions in the PC3 prostate and Bx-PC-3 pancreatic models, representing hard to treat cancers, following single cycles of treatment. Significant and long lasting tumor growth delays were observed in the other models tested including an advanced LS174T colon model where increases in lifespan of >40 days and superior activity to the standard drug irinotecan was achieved. Activity was observed in single i.v. and repeat dose (q4dx3 and qdx5) schedules. All studies tested a single cycle of treatment and there is clearly the potential for increased activity with repeated treatment cycles. In comparison with irinotecan, it is interesting to note that both compounds covalently link to bases on opposite DNA strands with a four base pair stagger.

The delivery of the PBD dimer SG2202 as a pro-drug has resulted in an agent (SG2285) with very different cellular and animal pharmacokinetic properties to SJG-136. Interestingly, despite the active cross-linking agent SG2202 being considerably more potent than SJG-136, the maximum tolerated dose of pro-drug SG2285 in mice is approximately 10-fold higher than for SJG-136. In LOX-IMVI and OVCAR-5 direct comparisons can be made between SG2285 and SJG-136 and in both cases SG2285 gave superior activity. For example, under the identical conditions used for SG2285 shown in Figure 4A, SJG-136 was highly active but produced cures in only 4/8 animals at its MTD (0.3 mg/kg), whereas SG2285 cured all animals (8/8) at 3 mg/kg, 6/8 animals at 1.5 mg/kg and 4/8 at 0.75 mg/kg. In the case of OVCAR-5, a single administration of SJG-136 at its MTD produced only a minimal growth delay, whereas SG2285 gave a significant tumor growth delay (Table 2).

The data suggest that the delivery of a highly active PDB as a pro-drug can result in an increased therapeutic index *in vivo*.

The diastereomeric ratio of SG2285 was found to be very sensitive to its method of synthesis, work-up and purification. For example, one set of conditions affords almost exclusively the 11*S*,11*S'* diastereomer (26.5:1 11*S*,11*S'*:11*S*,11'*R*) whereas different conditions can produce a 9:1 mixture in favour of the 11*S*,11'*R* diastereomer (17). Importantly, the ratio of C11/C11' diastereomers does not appear to influence *in vitro* cytotoxicity of SG2285 (data not shown). The present study also demonstrates that batches of drug with 11*S*,11*S'*:11*S*,11'*R* ratios ranging from 26.5:1 to 1:5.1 retain potent *in vivo* antitumor activity.

In summary, SG2285 is a novel C2-aryl substituted PBD dimer pro-drug with potent activity *in vitro* against human tumor cell lines and primary B-CLL cells, and *in vivo* against a wide range of human tumors, including those difficult to treat clinically. As a result of this impressive activity, SG2285 is in pre-clinical development towards Phase I clinical trials.

Supplementary Material

Refer to Web version on PubMed Central for supplementary material.

Acknowledgments

Spirogen Ltd (UK) is acknowledged for financial support of this project. Dr David Evans is thanked for the molecular model of SG2202 binding to DNA.

Grant Support:

Cancer Research UK programme grant C2259/A9994 to JAH and the UCL Experimental Cancer Medicine Centre.

REFERENCES

1. Thurston, DE. Advances in the study of pyrrolo[2,1-*c*][1,4]benzodiazepine (PBD) antitumor antibiotics. In: Neidle, S.; Waring, MJ., editors. *Molecular Aspects of Anticancer Drug-DNA Interactions*. The Macmillan Press Ltd; London: 1993. p. 54-88.
2. Hurley LH, Reck T, Thurston DE, et al. Pyrrolo(1,4)benzodiazepine antitumor antibiotics: relationship of DNA alkylation and sequence specificity to the biological activity of natural and synthetic compounds. *Chem Res Toxicol*. 1988; 1:258-68. [PubMed: 2979741]
3. Bose DS, Thompson AS, Ching J, et al. Rational design of a highly efficient irreversible DNA interstrand cross-linking agent based on the pyrrolobenzodiazepine ring system. *J Am Chem Society*. 1992; 114:4939-41.
4. Bose DS, Thompson AS, Smellie M, et al. Effect of linker length on DNA-binding affinity, cross-linking efficiency and cytotoxicity of C8-linked pyrrolobenzodiazepine dimers. *J Chem Soc Chem Commun*. 1992; 14:1518-20.
5. Thurston DE, Bose DS, Thompson AS, et al. Synthesis of sequence-selective C8-linked pyrrolo[2,1-*c*][1,4]benzodiazepine DNA interstrand crosslinking agents. *J Org Chem*. 1996; 61:8141-7. [PubMed: 11667802]
6. Gregson SJ, Howard PW, Hartley JA, et al. Design synthesis and evaluation of a novel pyrrolobenzodiazepine DNA-interactive agent with highly efficient cross-linking ability and potent cytotoxicity. *J Med Chem*. 2001; 44:737-8. [PubMed: 11262084]
7. Gregson SJ, Howard PW, Gullick DR, et al. Linker length modulates DNA crosslinking reactivity and potency for ether-linked C2-exo-unsaturated pyrrolo[2,1-*c*][1,4]benzodiazepine (PBD) dimers. *J. Med. Chem*. 2004; 47:1161-74. [PubMed: 14971896]

8. Smellie M, Kelland LR, Thurston DE, Souhami RL, Hartley JA. Cellular pharmacology of novel C8-linked anthramycin-based sequence-selective DNA minor-groove cross-linking agents. *Br J Cancer*. 1994; 70:48–53. [PubMed: 8018540]
9. Smellie M, Bose DS, Thompson AS, Jenkins TC, Hartley JA, Thurston DE. Sequence selective recognition of duplex DNA through covalent interstrand crosslinking: kinetic and molecular modelling studies with pyrrolobenzodiazepine (PBD) dimers. *Biochemistry*. 2003; 42:8232–9. [PubMed: 12846572]
10. Martin C, Ellis T, McGurk CJ, et al. Sequence-selective interaction of the minor-groove interstrand cross-linking agent SJG-136 with naked and cellular DNA: footprinting and enzyme inhibition studies. *Biochem*. 2005; 44:4135–47. [PubMed: 15766241]
11. Hartley JA, Spanswick VJ, Brooks N, et al. SJG-136 (NSC 694501), a novel rationally designed DNA minor groove interstrand cross-linking agent with potent and broad spectrum antitumor activity: Part 1: Cellular pharmacology, in vitro and initial in vivo antitumor activity. *Cancer Res*. 2004; 64:6693–9. [PubMed: 15374986]
12. Alley MC, Hollingshead MG, Pacula-Cox CM, et al. SJG-136 (NSC 694501), a novel rationally designed DNA minor groove interstrand cross-linking agent with potent and broad spectrum antitumor activity: Part 2: Efficacy evaluations. *Cancer Res*. 2004; 64:6700–6. [PubMed: 15374987]
13. Hochhauser D, Meyer T, Spanswick VJ, et al. Phase I study of a sequence selective minor groove DNA binding agent (SJG-136) with pharmacokinetic and pharmacodynamic measurements in patients with advanced solid tumors. *Clinical Cancer Res*. 2009; 15:2140–7. [PubMed: 19276288]
14. Puzanov I, Lee W, Berlin JD, et al. Final results of phase I and pharmacokinetic trial of SJG-136 administered on a daily x 3 schedule. *Proc. American Society of Clinical Oncology Annual Meeting. J. Clinical Oncology*. 2008; 26(15S) Abs 2512.
15. Janjigian YY, Lee W, Kris MG, et al. A phase I trial of SJG-136 (NSC694501) in advanced solid tumors. *Cancer Chemother. Pharmacol*. 2010; 65:833–8. [PubMed: 19672598]
16. Cooper N, Hagan DR, Tiberghien A, et al. Synthesis of novel C2-aryl pyrrolobenzodiazepines (PBDs) as potential antitumour agents. *Chem Commun*. 2002; 16:1764–5.
17. Howard PH, Chen Z, Gregson SJ, et al. Synthesis of a novel C2/C2'-aryl-substituted pyrrolo[2,1-c]-[1,4]benzodiazepine dimer prodrug with improved water solubility and reduced DNA reaction rate. *Bioorganic Med. Chem. Lett*. 2009; 19:6463–6.
18. Clingen PH, De Silva IU, McHugh PJ, et al. The XPF-ERCC1 endonuclease and homologous recombination contribute to the repair of minor groove DNA interstrand crosslinks in mammalian cells produced by the pyrrolo[2,1-c][1,4]benzodiazepine dimer SJG-136. *Nucleic Acids Res*. 2005; 33:3283–91. [PubMed: 15944449]
19. Hartley JM, Spanswick VJ, Gander M, et al. Measurement of DNA crosslinking in patients on ifosfamide therapy using the single cell gel electrophoresis (comet) assay. *Clin Cancer Res*. 1999; 5:507–12. [PubMed: 10100700]
20. Spanswick, VJ.; Hartley, JM.; Ward, TH.; Hartley, JA. Measurement of drug-induced DNA interstrand crosslinking using the single cell gel electrophoresis (comet) assay. In: Brown, R.; Boger-Brown, U., editors. *Methods in Molecular Medicine, Vol. 28: Cytotoxic Drug Resistance Mechanisms*. Humana Press; New York: 1999. p. 143-54.
21. Pepper C, Thomas A, Hidalgo de, Quintana J, Davies S, Hoy T, Bentley P. Pleiotropic drug resistance in B-cell chronic lymphocytic leukaemia – the role of Bcl-2 family proteins. *Leukemia Research*. 1999; 23:1007–14. [PubMed: 10576505]
22. Cartwright R, Tambini CE, Simpson PJ, Thacker J. The XRCC2 DNA repair gene from human and mouse encodes a novel member of the recA/RAD51 family. *Nucleic Acids Res*. 1998; 26:3084–9. [PubMed: 9628903]
23. Liu N, Lamerdin JE, Tebbs RS, et al. XRCC2 and XRCC3, new human Rad51-family members, promote chromosome stability and protect against DNA cross-links and other damages. *Mol. Cell*. 1998; 1:783–93. [PubMed: 9660962]
24. Yamada NA, Hinz JM, Kopf VL, Segalle KD, Thompson LH. XRCC3 ATPase activity is required for normal XRCC3-Rad51C complex dynamics and homologous recombination. *J. Biol. Chem*. 2004; 279:23250–4. [PubMed: 15037616]

25. Yokoyama H, Sarai N, Kagawa W, et al. Preferential binding to branched DNA strands and strand-annealing activity of the human Rad51B, Rad51C, Rad51D and Xrcc2 protein complex. *Nucleic Acids Res.* 2004; 32:2556–65. [PubMed: 15141025]
26. Kuraoka I, Kobertz WB, Ariza RR, Biggerstaff M, Essigmann JM, Wood RD. Repair of an interstrand DNA cross-link initiated by ERCC1-XPF repair/recombination nuclease. *J. Biol. Chem.* 2000; 275:26632–6. [PubMed: 10882712]
27. De Silva IU, McHugh PJ, Clingen PH, Hartley JA. Defining the roles of nucleotide excision repair and recombination in the repair of DNA interstrand cross-links in mammalian cells. *Mol Cell Biol.* 2000; 20:7980–90. [PubMed: 11027268]
28. De Silva IU, McHugh PJ, Clingen PH, Hartley JA. Defects in interstrand cross-link uncoupling do not account for the extreme sensitivity of ERCC1 and XPF cells to cisplatin. *Nucleic Acids Res.* 2002; 30:3848–56. [PubMed: 12202770]
29. McHugh PJ, Spanswick VJ, Hartley JA. Repair of DNA interstrand crosslinks: molecular mechanisms and clinical relevance. *Lancet Oncol.* 2001; 2:483–90. [PubMed: 11905724]
30. Pepper CJ, Hambly RM, Fegan CD, Delavault P, Thurston DE. The novel sequence-specific DNA cross-linking agent SJG-136 (NSC 694501) has potent and selective in vitro cytotoxicity in human B-cell chronic lymphocytic leukemia cells with evidence of a p53-independent mechanism of cell kill. *Cancer Res.* 2004; 64:6750–5. [PubMed: 15374993]
31. Lee JS, Dixon DO, Kantarjian HM, Keating MJ, Talpaz M. Prognosis of chronic lymphocytic leukemia: a multivariate regression analysis of 325 untreated patients. *Blood.* 1987; 69:929–36. [PubMed: 3814821]
32. Hartley JA, Martin C, Hamaguchi A, et al. SG2285, a novel C2-aryl-substituted pyrrolobenzodiazepine dimer prodrug with potent antitumor activity. *Proc AACR.* 2008; 49 Abs 3302.

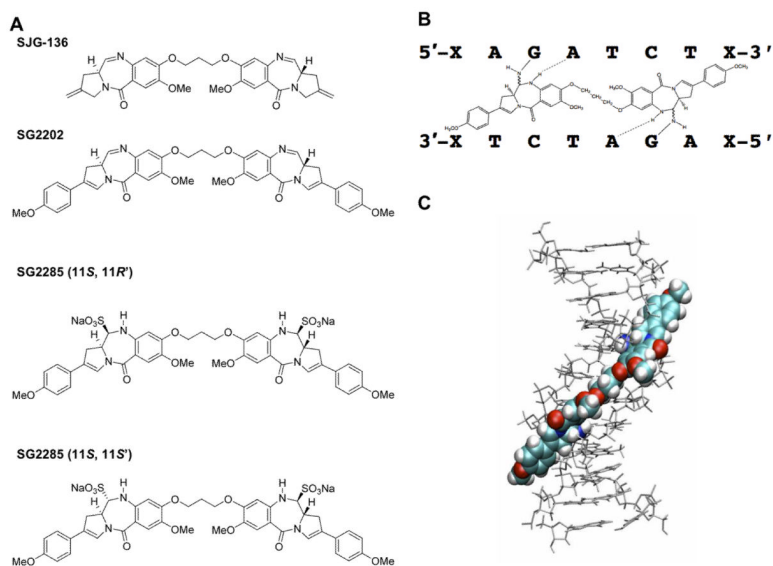


Figure 1.

A. Structures of SJG-136 (SG2000), SG2202 and SG2285. SG2285 is shown in the 11*S*, 11'*R* and 11*S*,11'*S* diastereomeric forms. B. Scheme of SG2202 binding across eight base pairs in the DNA sequence 5'-XAGATCTX-3', forming a DNA interstrand cross-link between guanine N2 groups spanning four base pairs. C. Molecular model of SG2202 binding in the DNA minor groove.

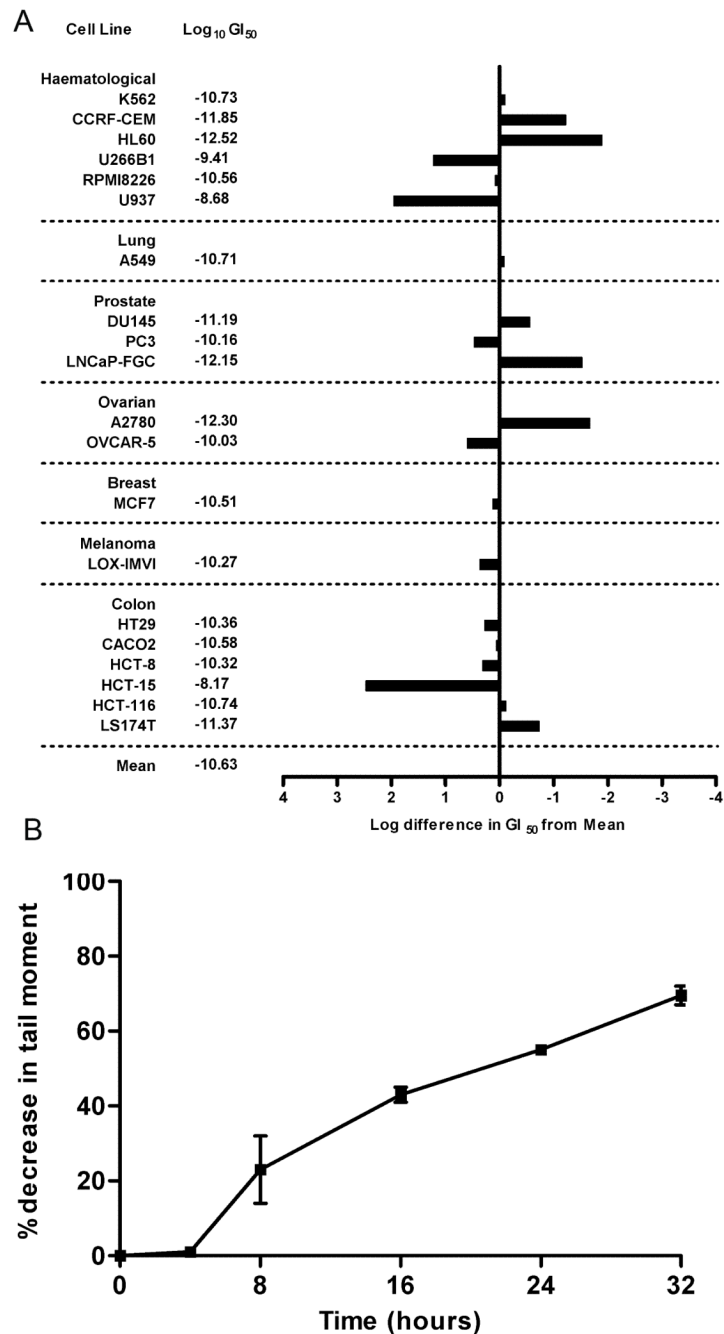


Figure 2.

A. Averaged mean graphs for the cytotoxicity of SG2285 against a panel of human tumor cell lines. The figure provides a graphic and tabular listing of the molar drug concentrations (log units) conferring 50% net growth inhibition (GI₅₀) for each cell line. The response of each cell line relative to the mean of all cell line responses is depicted by a horizontal bar extending either to the right (more sensitive) or to the left (less sensitive) of the mean (vertical line). The length of each bar is proportional to the cell line sensitivity relative to the mean. B. DNA interstrand cross-link formation in the human prostate cancer cell line DU-145 following treatment with 1 nM SG2285. Cross-linking, expressed as the % decrease in tail moment compared to irradiated control non-drug treated cells, was determined using

the single cell gel electrophoresis (comet) assay. Data are the mean \pm s.d. of three independent experiments (the individual experimental data are shown in the Supplementary Material section S4).

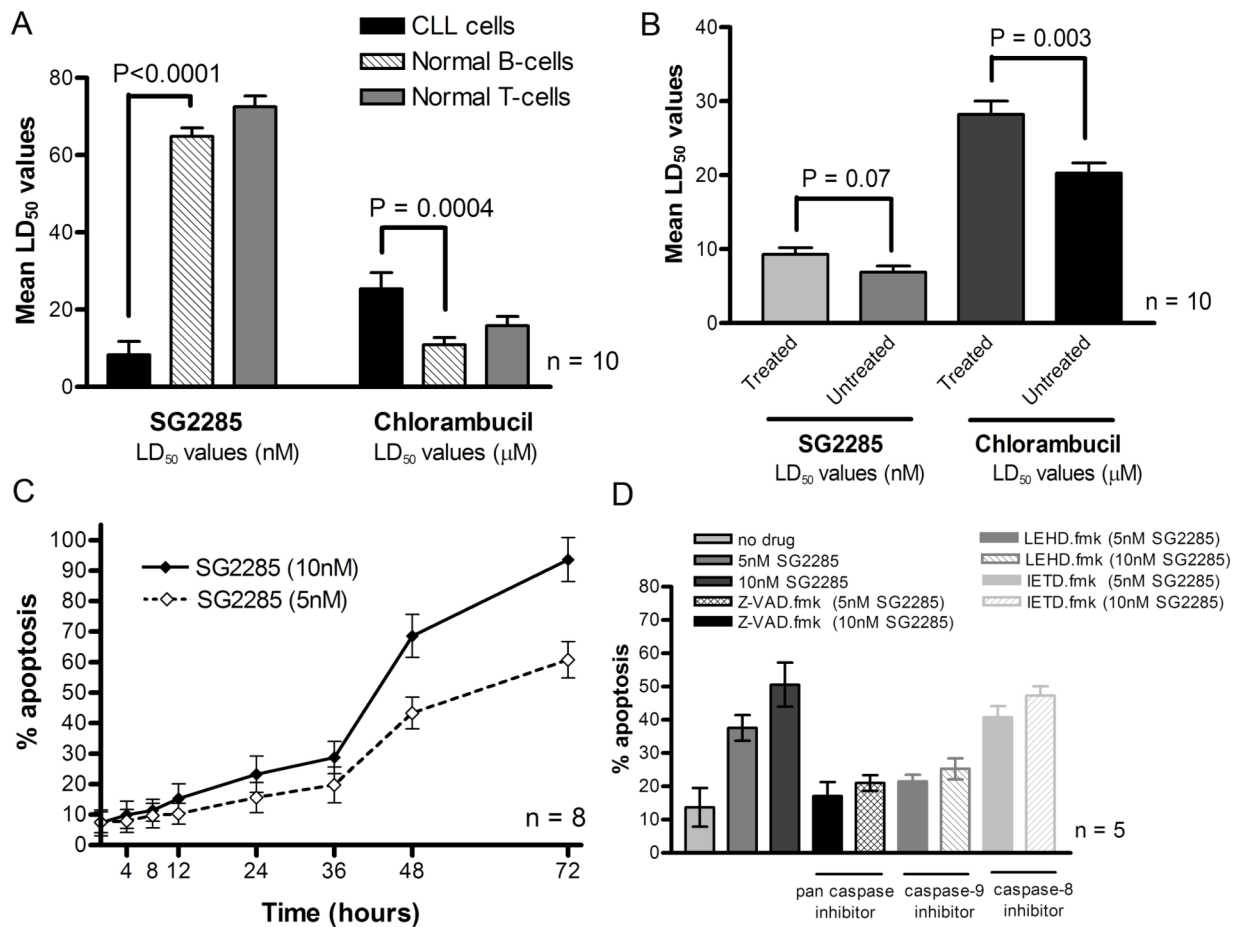


Figure 3.

A. Cytotoxicity of SG2285 or chlorambucil expressed as LD₅₀ values (\pm SD) derived from *in vitro* primary B-CLL samples from 20 patients and B- and T-lymphocyte subsets from 10 normal age-matched control samples. Data are mean \pm SD. B. Comparison of LD₅₀ values (mean \pm SD) for SG2285 or chlorambucil in samples derived from previously treated (n=10) and untreated (n=10) CLL patients. C. Kinetics of apoptosis induction in primary B-CLL cells treated with 5 and 10 nM SG2285. D. Effect of caspase inhibitors on apoptosis in B-CLL cells following exposure to SG2285 for 48h. Results are the mean (\pm SD) of three separate experiments.

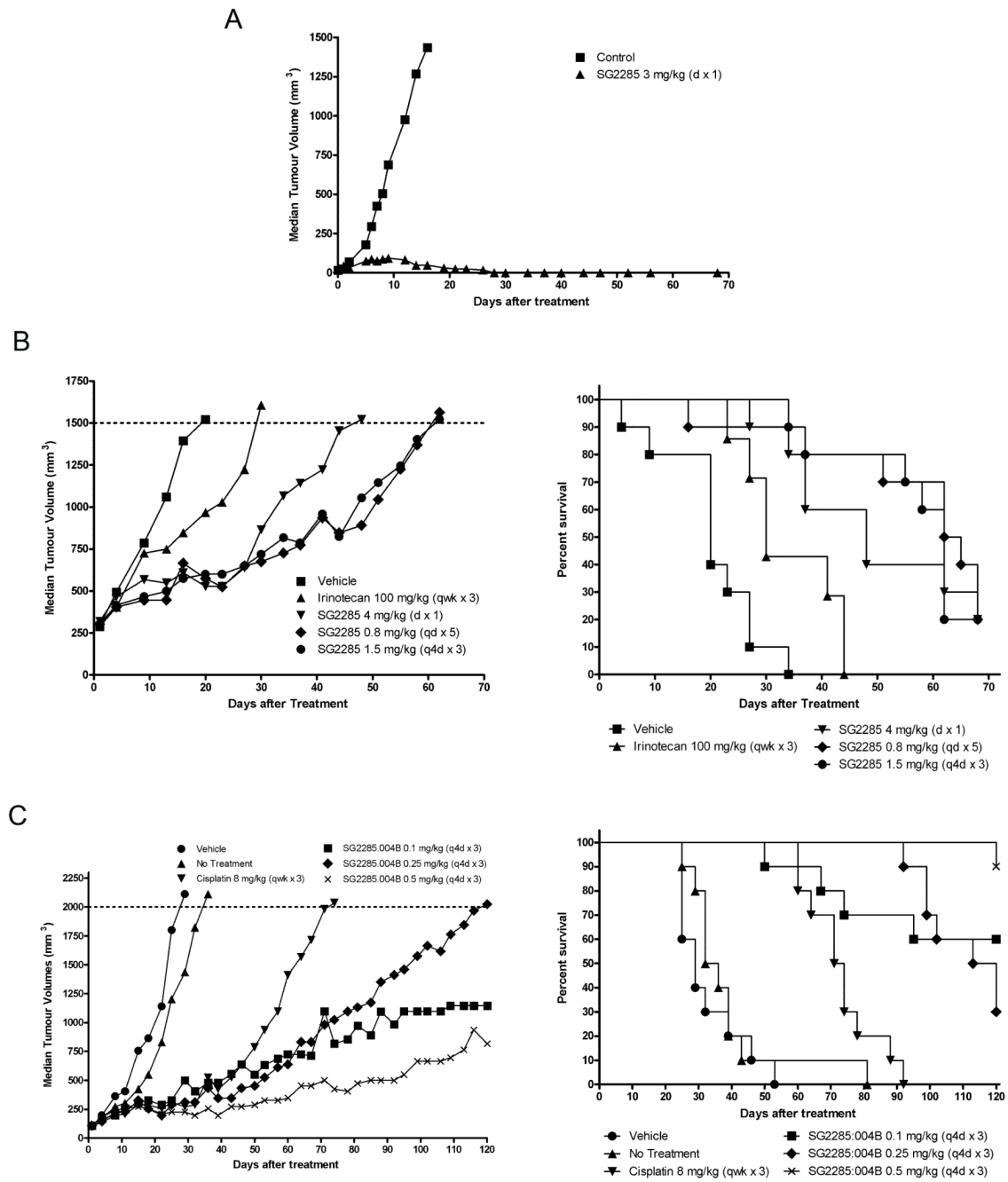


Figure 4. Representative *in vivo* human tumor xenograft experiments following treatment with SG2285. A. Tumor growth curves for single i.v. exposure to LOX-IMVI human melanoma. Data are from 7 animals in each group resulting in 7/7 tumor free survivors at day 68. B. Tumor growth curves (left) and Kaplan-Meier plots (right) for the advanced LS174T human colon tumor model following treatment with SG2285 at three different schedules (4 mg/kg dx1, 0.8 mg/kg qdx5, 1.5 mg/kg q4dx3). Irinotecan (100 mg/kg qwkx3) is included for comparison. Data are from 10 animals/ group. C. Tumor growth curves (left) and Kaplan-Meier plots (right) for the SKOV-3 human ovarian tumor model following treatment with

SG2285 q4dx3 at 0.1, 0.25 and 0.5 mg/kg. Cisplatin (8 mg/kg qwkx3) is included for comparison.

Table 1
GI50 values for SG2285 in Chinese hamster ovary wild type and DNA repair defective mutant cell lines

Cell Line	Parent	Defective Gene	Repair Pathway ^a	GI ₅₀ ± SEM (nM)	S.R. ^b
AA8	-	-	-	2.17 ± 1.17	-
UV23	AA8	XPB	NER	1.83 ± 0.17	1.2
UV47	AA8	XPF	NER	0.70 ± 0.40	3.1
UV61	AA8	CSB	NER	0.73 ± 0.15	3.0
UV96	AA8	ERCC1	NER	0.18 ± 0.04	12.1
UV135	AA8	XPG	NER	0.67 ± 0.15	3.2
irs1SF	AA8	XRCC3	HRR	0.20 ± 0.10	10.9
V79	-	-	-	3.17 ± 0.17	-
irs1	V79	XRCC2	HRR	0.19 ± 0.08	16.7
CHO-K1	-	-	-	0.23 ± 0.06	-
xrs5	CHO-K1	XRCC5	NHEJ	0.52 ± 0.39	0.4

^aNER - nucleotide excision repair, HRR – homologous recombination repair, NHEJ – non-homologous end joining

^bS.R. – sensitivity ratio compared to wild type

Table 2. A

Summary of *in vivo* data for SG2285 in human tumor xenograft models LOX-IMVI (melanoma), advanced LS174T (colon), OVCAR-5 (ovarian) and SKOV-3 (ovarian)

Model	Tumor Type	Dose (batch) (mg/kg)	Schedule (i.v.)	Duration (days)	%TGD ¹	CR (TFS) ²
LOX-IMVI	Melanoma	3 (1)	d × 1	68	n/a	7/7 (7/7)
LOX-IMVI	Melanoma	3 (1)	d × 1	86	n/a	8/8 (8/8)
		1.5 (1)	d × 1	86		6/8 (6/8)
		0.75 (1)	d × 1	86		4/8 (4/8)
Advanced LS174T3	Colon	4 (2)	d × 1	69	138	-
		1.5 (2)	q4d × 3	69	219	-
		0.8 (2)	qd × 5	69	202	-
OVCAR-5	Ovarian	3 (1)	d x1	56	59	-
SKOV-3	Ovarian	0.8 (2)	qd × 5	79	168	1/8 (1/8)
		0.4 (2)	qd × 5	79	77	1/8 (1/8)
		0.2 (2)	qd × 5	79	63	-
		1.5 (2)	q4d × 5	79	229	1/8 (1/8)-
		0.75 (2)	q4d × 5	79	129	1/8 (1/8)
		0.375 (2)	q4d × 5	79	85	-
SKOV-3	Ovarian	0.1 (3)	q4d × 3	120	325	-
		0.25 (3)	q4d × 3	120	309	-
		0.5 (3)	q4d × 3	120	325	-
		0.2 (4)	q4d × 3	120	156	1/8 (1/8)
		0.5 (4)	q4d × 3	120	180	-
		1.0 (4)	q4d × 3	120	248	-

¹ %TGD = % tumour growth delay = [(T-C)/C] × 100

² CR = total number of complete regressions, TFS = tumor free survivors (i.e. CRs at end of study)

³ Irinotecan (100 mg/kg i.p. qwk × 3) gave %TGD of 54 in this experiment (see figure 4B)

B

Summary of *in vivo* data for SG2285 and appropriate standard agents in human tumor xenograft models LS174T (colon), A549 (non small cell lung), PC3 (prostate) and Bx-PC-3 (pancreatic).

Model	Drug	Dose (batch) (mg/kg)	Schedule ¹	Duration (days)	%TGI ²	PR ³
LS174T (colon)	SG2285 Irinotecan 5-FU	0.85 (3)	q4d × 3	26	83	0
		1.0 (3)	q4d × 3	26	82	0
		100	qwk × 3 (ip)	26	46	0
		100	qwk × 3 (ip)	26	65	0
A549 (NSCLC)	SG2285 Docetaxel	1.0 (5)	q4d × 4	29	63	0
		30	q4d × 3	29	89	0
PC3 (prostate)	SG2285 Paclitaxel Cisplatin	0.75 (5)	q4d × 4	30	96	5/10
		1.0 (5)	q4d × 3	30	96	4/10
		30	qod × 5	30	99	8/10
		10	qwk × 3 (ip)	30	72	0
Bx-PC-3 (pancreatic)	SG2285 Paclitaxel	1.0 (3)	q4d × 4	30	86	2/9
		1.0 (3)	q4d × 3	30	69	1/9
		1.0 (5)	q4d × 4	30	81	1/8
		1.0 (5)	q4d × 3	30	84	2/8
		30	qod × 5	30	47	0

¹ Drug given i.v. unless indicated otherwise

² %TGI = $[1 - (T/C)] \times 100$ = % tumor growth inhibition compared to vehicle controls. TGI 60% indicates therapeutic activity.

³ PR = partial regression (tumor volume 50% or less than its day 1 volume for three consecutive measurements)